Chloride Channel Function in the Yeast TRK-Potassium Transporters

T. Kuroda[1,2], H. Bihler[3], E. Bashi[1], C. L. Slayman[1], A. Rivetta[1]

[1]Department of Cellular and Molecular Physiology, Yale School of Medicine, 333 Cedar Street, New Haven, CT 06520, USA
[2]Department of Microbiology, Faculty of Pharmaceutical Sciences, Okayama University, Okayama, 700-8530, Japan
[3]Botanisches Institut, Lehrstuhl I, Universität Karlsruhe, D-76128, Karlsruhe, Germany

Abstract. The TRK proteins—Trk1p and Trk2p—are the main agents responsible for "active" accumulation of potassium by the yeast *Saccharomyces cerevisiae*. In previous studies, inward currents measured through those proteins by whole-cell patch-clamping proved very unresponsive to changes of extracellular potassium concentration, although they did increase with extracellular proton concentration—qualitatively as expected for H^+ coupling to K^+ uptake. These puzzling observations have now been explored in greater detail, with the following major findings: a) the large inward TRK currents are not carried by influx of either K^+ or H^+, but rather by an efflux of chloride ions; b) with normal expression levels for Trk1p and Trk2p in potassium-replete cells, the inward TRK currents are contributed approximately half by Trk1p and half by Trk2p; but c) strain background strongly influences the absolute magnitude of these currents, which are nearly twice as large in W303-derived spheroplasts as in S288c-derived cells (same cell-size and identical recording conditions); d) incorporation of mutations that increase cell size (deletion of the Golgi calcium pump, Pmr1p) or that upregulate the *TRK2* promoter, can further substantially increase the TRK currents; e) removal of intracellular chloride (e.g., replacement by sulfate or gluconate) reveals small inward currents that are K^+-dependent and can be enhanced by K^+ starvation; and f) finally, the latter currents display two saturating kinetic components, with preliminary estimates of $K_{0.5}$ at 46 μM $[K^+]_{out}$ and 6.8 mM $[K^+]_{out}$, and saturating fluxes of ~5 mM/min and ~10 mM/min (referred to intracellular water). These numbers are compatible with the normal K^+-transport properties of Trk1p and Trk2p, respectively.

Introduction

Whereas most living cells retain a single ionic species, potassium, as the predominant intracellular cation, they have evolved at least three different classes of mechanism to sustain that high intracellular K^+. Among animal cells, the principal mechanism is exchange of sodium for potassium via the well-known Na^+, K^+-ATPase, which—because of its transport asymmetry, 3 Na^+/2 K^+—generates an efflux of (+) charges, thereby contributing a small component of the resting membrane voltage (*see* Slayman, 1982; Blaustein & Lieberman, 1984; Läuger, 1991). However, in almost all other kinds of cells: plants, fungi, and bacteria, potassium accumulation is mainly *driven* by the membrane voltage, which in most cases arises from an ATP-fueled forced extrusion of protons. In these systems, the resultant membrane voltages are sometimes very large (150–300 mV, cell interior negative), so that K^+ accumulation ratios of ~3×10^2 to nearly 10^5 might be achieved, in principle, by passive flux through K^+-selective channels in the plasma membrane. This fact, indeed, has been widely employed for cloning and/or mutagenesis of heterologous potassium channels in yeast (Anderson et al., 1992; Sentenac et al., 1992; Goldstein et al., 1996; Minor et al., 1999).

But conventional ion channels, per se, are not the sole route for potassium accumulation, even in the high-voltage cells of plants, fungi, or bacteria. Rather, at least three quite different classes of proteins are involved, in different species of cells. All three are represented in certain bacteria, such as *Escherichia coli* (Bakker, 1993a; Stumpe et al., 1996):

these are (*i*) an inducible K⁺-ATPase (designated Kdp-ATPase), which resembles the Na⁺,K⁺-ATPase in reaction chemistry, but is structurally quite distinct, and which explicitly pumps potassium ions inward without coupling to sodium extrusion; (*ii*) a constitutive, non-ATP-dependent carrier (Kup), which is widely regarded as a proton-coupled transporter, and whose primary sequence suggests it to possess 12 transmembrane helices, like the majority of proton-coupled substrate transporters (Schleyer & Bakker, 1993; Bañuelos et al., 1995); and (*iii*) a second type of constitutive carrier (TrkG,H), which has recently been shown to fold like a potassium channel, with 4 pairs of transmembrane helices, each pair bracketing a recurrent loop (P-loop) that protrudes into the membrane from the extracellular surface (Durell & Guy, 1999; Tholema et al., 1999; Uozumi et al., 2000; Kato et al., 2001; Haro & Rodriguez-Navarro, 2002, 2003; Zeng, Pypert & Slayman, 2004).

The latter class of proteins provides the principal mechanism for potassium uptake by the yeast *Saccharomyces cerevisiae*, which possesses two members: Trk1p, a high-affinity transporter (K_m ∼30 μM K⁺); and Trk2p, a moderate-affinity transporter (K_m ∼10 mM K⁺). The Kdp- and Kup-class transporters are absent from *Saccharomyces*. Although the functional literature on Trk1p and Trk2p is skeltered and rather confusing, both transporters appear to be two-ion carriers in which one binding site is highly specific for potassium, while the second accommodates a variety of cations: K⁺, Na⁺, H⁺, etc., depending on what is present (Armstrong & Rothstein, 1964, 1967; Haro et al., 2002). This view is consistent not only with a wide range of kinetic studies on yeast, but also—for Trk1p—with the finding of K⁺-H⁺ coupling in high-affinity K⁺ uptake by the related ascomycete, *Neurospora* (Rodriguez-Navarro, Blatt & Slayman, 1986; Blatt, Rodriguez-Navarro & Slayman, 1987); and with many recent kinetic measurements on other TRK-family proteins in bacteria (Bakker, 1993b; Schlösser et al., 1995; Tholema et al., 1999) and in higher plants (Rubio et al., 1995, 1999; Diatloff, Kumar & Schachtman, 1998; Liu, Schachtman & Zhang, 2000; Uozumi et al., 2000).

Most ion transporters and ion-coupled transporters move net charges through biological membranes, and in consequence produce electrical signals. Bihler et al. (1999) took advantage of this fact to initiate a detailed functional study of the TRK proteins in yeast by means of patch recording. The major findings of that initial work were the following:

1) The TRK proteins, taken together (in wild-type yeast) behave like an inward rectifier, letting progressively larger currents flow toward the cell interior, as membrane voltage is clamped progressively negative to −100 mV.

2) These inward currents are enhanced by increasing the extracellular proton concentration (lowering pH$_o$), but plots of current versus voltage—so-called *I-V* plots—retain a constant shape, and simply slide in the positive direction along the voltage axis, displaying increased currents at any fixed voltage, as pH$_o$ falls.

3) The currents develop almost instantaneously with appropriate voltage steps, and show no time-dependent increase or decrease, which usually characterizes voltage-gated ion channels.

4) The currents are remarkably insensitive to extracellular potassium, showing no significant change when the concentration ([K⁺]$_o$) is shifted between nearly zero (stray K⁺, ∼10 μM) and 150 mM.

5) The currents are quite large for normal-sized yeast cells, in the range of 100 pA at −200 mV, compared with expected (H⁺) currents through the proton pump of ∼20 pA.

6) The currents had appeared associated with the low-affinity transporter, Trk2p, rather than with the high-affinity transporter, Trk1p, as had been expected after the demonstration of K⁺ currents through a high-affinity potassium transporter in the related ascomycete, *Neurospora crassa* (Rodriguez-Navarro et al., 1986; Blatt et al., 1987).

While the first three of these observations seem reasonably related to the known biological function of the TRK proteins in yeast, the last three, especially (4) and (5), are difficult to reconcile with that function. The present experiments were therefore undertaken to characterize the TRK currents in more detail, and to try to understand features 4–6 especially. The most important new result, then, is that the conspicuous inward TRK currents measured under customary conditions for yeast patch-clamping are in fact dependent upon intracellular *anions*, especially chloride. They are also supported by both Trk1p and Trk2p, but are strongly dependent upon the strain background of the yeast cells studied. In short, the yeast TRK proteins have properties and functions that are quite distinct from their role in potassium uptake and regulation.

Materials and Methods

Strains, Media, and Buffers

Table 1 lists the yeast strains for these experiments, along with their genotypes and sources. Strain K837 (Cunningham) was constructed as described by Locke et al. (2000), starting with W303-1A. The diploid strain AB541 (Gaber) was made by mating the haploid parents indicated in Table 1, which were constructed in the S288c background by the methods of Gaber, Styles & Fink (1986) and of Vidal et al. (1990, 1995). The isogenic set of haploid TRK-deletion strains in the S288c background, designated PLY232, ..., PLY256 in Table 1, were constructed in the Ljungdahl laboratory by methods described in Bertl et al. (2003).

Table 1. Yeast strains used

Strain name	Genotype	Source
BS202/203[1]	*MAT**a**/α ade2-1 can1-100 his3-11,15 leu2-3,112 trp1-1 ura3-1 lys2-ΔNhel* (W303 background)	Bert Smith, in S. Roeder laboratory
EBC202/203	BS202/203 → *pmr1Δ::TRP1*	Esther Bashi, in this laboratory
EBE202/203	BS202/203 → *trk1Δ::TRP1*	idem
EBF202/203	BS202/203 → *trk2Δ::TRP1*	idem
EBH202	BS202 → *trk1Δ::TRP1 pmr1Δ::TRP1*	idem
EBJ202	BS202 → *trk2Δ::TRP1 pmr1Δ::TRP1*	idem
EBK202	BS202 → *trk1Δ::TRP1 trk2Δ::TRP1 pmr1Δ::TRP1*	idem
K837	*MAT**a** ade2-1 can1-100 his3-11,15 leu2-3,112 trp1-1 ura3-1 URA3::pmc1-lacZ pmr1::HIS3 + pKC217 plasmid* (W303 background)	Kyle Cunningham
AB541[2]	*MAT**a** lys9 HIS4 trk1Δ1 trp1Δ1 ura3-52 RPD2-5* *MATα LYS9 his4-15 trk1Δ1 TRP1 ura3-52 RPD2-5* (S288c background, diploid, *TRK2* upregulated)	Richard Gaber
PLY232/248	*MAT**a**/α his3-Δ200 leu2-3,112 trp1-Δ901 ura3-52 suc2-Δ9* (S288c background)	Per Ljungdahl
PLY234/250	PLY232/248 → *trk1-Δ51*	idem
PLY236/252	PLY232/248 → *trk2-Δ50::lox-kanMX-lox*	idem
PLY240/256	PLY232/248 → *trk1-Δ51 trk2-Δ50::lox-kanMX-lox*	idem

[1] Designations like BS202 and BS203 denote strains isogenic except for mating type, and the numbers correspond to *MAT**a*** and *MATα*, in the same order; viz., BS202 is *MAT**a***, and BS203 is *MATα*. Similarly, PLY234 and PLY250 are *MAT**a*** and *MATα*, respectively.
[2] This strain, only, is diploid; all of the others are haploid.

The isogenic set of haploid TRK1,2- and PMR1-deletion strains in the W303 background, designated EB**X**202 (*MAT**a***) and EB**X**203 (*MATα*.) in Table 1, were constructed as follows. The single-deletion strains (EBC. . ., EBE. . ., and EBF. . .) were created via homologous recombination and selected on tryptophan-negative medium, after transformation of BS202 and BS203 with DNA made by PCR from plasmid pRS304 (*TRP1* marker; Sikorski & Hieter, 1998). The following paired PCR primers were used: (*upper case* = homing sequence in the respective yeast gene; *lower case* = plasmid sequence flanking *TRP1*):

For *trk1Δ*:
CTAACAATGCATTTTAGAAGAACGATGAGTAGAGT GCCCACATTGGCgcgtttcggtgatgacgg and CTCCTTTTAGGA TTTCGGGAATGTGTGGTCTTACGCTTAAGAGCTCtagggtg atggttcacgtagtg, which left intact 13 *TRK1* codons 5′ of the *TRP1* insert and 20 codons 3′ of the insert.

For *trk2Δ*:
GCTATTTTGTACTATTCACCGACGATAAGAGGCTG TAAGAACCACTCgcgtttcggtgatgacgg and CGTTGGCTCTTA TGTAGGTAAAGAGGGGTAAACTTGATTTTAATGtagggtga tggttcacgtagtg, which left intact only two codons at the 3′ end of *TRK2*.

For *pmr1Δ*:
GCAAGACAAGACGAAGCAAGGCCAGCACAGACGT AAGCTTAAGTGTgcgtttcggtgatgacgg and GTACATTTACCTC AATAGGGTTGGGCGTCCTCATGAAAGATAtagggtgatggttca cgtagtg,which left no *PMR1* codons flanking the *TRP1* insert.

The final deletion constructs were verified by independent sequencing. The double-and triple-deletion strains (EBH. . ., EBJ . . ., EBK. . .) were made by mating the appropriate single-deletion strains, sporulating the diploids, dissecting complete asci, screening the tetrads, first for growth/no growth on low K⁺, and second, for DNA size across the regions of each of the three genes. *pmr1Δ*

strains were easily identified morphologically, by formation of conspicuously large cells during growth on agar plates. Finally, each of the EB**X**. . . strains in Table 1 was checked for spurious copies of the deleted genes by PCR of genomic DNA with primers from within the deleted regions.

For most experiments, cells were grown in shaking liquid YPD medium (0.5% yeast extract, 0.5% bactopeptone, 2% glucose), at 30°C, to an optical density of 0.8–1.2. For strains carrying the *pmr1Δ* mutation, 10 mM CaCl₂ was added to the growth medium; and for *trk1Δ* strains, 90 mM KCl was added to the growth medium. The standard buffers used for preparing, stabilizing, and recording from yeast spheroplasts are listed in Table 2, along with the standard pipette (intracellular) solution. Variations from these standard solutions—for the purpose of adding inhibitors, substituting specific ions, or changing pH—are stated in the applicable figure and table legends.

KSM (K⁺-starvation medium) was based on the arginine-phosphate medium of Rodriguez-Navarro & Ramos (1984), and contained 10 mM arginine, brought to pH 6.5 with phosphoric acid, 2% glucose, 3 mM NaCl, 1 mM CaCl₂, 1 mM MgCl₂, 0.35 mM adenine, vitamins, trace elements, and the full amino-acid mix as in synthetic complete medium (Sherman, 1991), plus 50 μM KCl for EBC202 or 10 mM KCl for EBK202.

Growth Experiments

Quantitative growth experiments were carried out in 24-well microtiter plates, each set up with 6 yeast strains and 4 potassium concentrations, in duplicate. Cells were harvested from overnight cultures grown to O.D. ∼1, pelleted, rinsed, resuspended in distilled water, and injected into the appropriate wells at 0.03 O.D., then incubated on a reciprocating shaker at 30°C. O.D. measurements (at

Table 2. Buffer solutions

Name	Composition
Buffer A (wash buffer)	50 mM KH_2PO_4 titrated to pH 7.2 with KOH, 0.2% β-mercaptoethanol (β-ME)
Buffer B (spheroplasting buffer)	Buffer A + 1.2 M sorbitol + 0.6 Units/ml zymolyase 20T (# 320921, ICN Biomedicals Inc., Irvine CA)
Buffer C (stabilizing buffer)	220 mM KCl, 10 mM $CaCl_2$, 5 mM $MgCl_2$, 5 mM MES titrated to pH 7.2 with Tris base + 0.2% glucose
Buffer D (sealing buffer)	150 mM KCl, 10 mM $CaCl_2$, 5 mM $MgCl_2$, 1 mM MES titrated to pH 7.5 with Tris base
Buffer 5.5	150 mM KCl, 10 mM $CaCl_2$, 5 mM $MgCl_2$, 1 mM MES titrated to pH 5.5 with Tris base
Buffer 4.5	150 mM KCl, 10 mM $CaCl_2$, 5 mM $MgCl_2$ 1 mM DMG titrated to pH 4.5 with Tris base
Buffer G (whole-cell pipette sol.)	175 mM KCl, 1 mM EGTA, 0.15 mM $CaCl_2$ 4 mM $MgCl_2$ 4 mM ATP titrated to pH 7.0 with KOH

MES: 2-(N-morpholino) ethanesulfonic acid.
DMG: 3,3′-dimethylglutaric acid.

600 nm) were made on a FLUOstar Galaxy microtiter plate reader (BMG-Labtechnologies, Offenburg, Germany), periodically until early stationary phase was reached. The optical density readings were then transferred to a templated Excel spread sheet. Scatter in the measurements was minimized by duplicate plates for each condition and duplicate readings of each well at each time point.

PATCH-CLAMP EXPERIMENTS

We used the whole-cell recording mode, essentially by the standard methods already described for yeast (Bertl et al., 1998), though with modifications of the buffer solutions, as listed in Table 2. Otherwise, the following slightly modified procedures were used.

Spheroplasting

This was carried out on 4–5 O.D. × ml of cells from late exponential-phase liquid cultures (*see* above). Cells were harvested by centrifugation, washed twice in 3 ml of Buffer A, but without β-mercaptoethanol (β-ME; Table 2). The resulting pellet was resuspended in 3 ml of Buffer A containing 0.2% β-ME and incubated at 30°C for 30 min on a slow orbital shaker (64 rpm). After recentrifugation, the cells were resuspended in 6 ml of Buffer B containing zymolyase, and incubated at 30°C for 45 min. The resulting spheroplasts were pelleted, gently resuspended in 5 ml of Buffer C and maintained at room temperature (∼23 °C) for use. In each test run, 1.5–3.0 μl of spheroplast suspension was gently injected onto the bottom of the recording chamber (700 μl volume), and cells were allowed ∼10 min to settle and adhere lightly to the chamber bottom. Gigaseal formation and whole-cell recording were achieved as described below for Figure 1.

Preparation of K⁺-starved Cells

K⁺-starved cells were used in the experiments of Figs. 8 and 9. Two steps were necessary to reveal TRK-mediated potassium currents: lowering of intracellular (pipette) chloride to the range of 1 mM or less, and sustained but limited K⁺-starvation of the cells. The two strains that were studied in such a Cl⁻- and K⁺-depleted state were EBC202 (*TRK1 TRK2 pmr1*Δ) and EBK202 (*trk1*Δ *trk2*Δ *pmr1*Δ), and both were K⁺-starved by incubation of cells in K⁺-starvation medium (KSM) for 12 h following growth in YPD (EBC202) or in 90 mM-K⁺-supplemented YPD medium (EBK202). At the end of KSM-incubation, aliquots of cells were harvested, filtered, rinsed, and assayed by flame-emission spectrophotometry, which showed them to contain potassium below 100 mMoles/kg cell water (cf.

normal values near 200 mMoles/kg cell water). Spheroplasting was carried out as above, except that KSM was substituted for potassium phosphate, in Buffers A and B; and KSM + 350 mM sorbitol replaced Buffer C. Low-K⁺ sealing buffer, which replaced Buffer D, contained 10 mM calcium gluconate, 5 mM magnesium gluconate, 1 mM MES brought to pH 5.5 with dimethylglutaric acid, 270 mM sorbitol, and 50 μM KCl. When [K⁺]$_{out}$ was raised, to assess K⁺-dependent currents, osmotically equivalent sorbitol was removed from the sealing buffer. Low-K⁺ pipette solution, replacing Buffer G, contained 14 mM potassium gluconate, 1 mM EGTA, 0.59 mM $CaCl_2$, 0.5 mM $MgCl_2$, 4.25 mM magnesium gluconate, 287 mM sorbitol, 4 mM K_2ATP, plus KOH to pH 7.0. The critical intracellular ions were: [K⁺] at ∼30 mM, [Cl⁻] at ∼1.2 mM, and free Ca^{++} at ∼110 nM. Whole-cell patch recording was achieved as described below, except with low-K sealing buffer instead of Buffer D.

Patch Recording

Pipettes were made of borosilicate glass (Kimax-51 Kimble/Kontes 38500), drawn on a two-stage puller (Narishige, model PC-10), and heat-polished on an electric microforge. The resulting pipettes were filled with Buffer G (Table 2) and had tip resistances of 3–5 MΩ when dipped into Buffer D (sealing buffer, Table 2); or slightly higher resistances, 6–9 MΩ, when chloride in Buffer G was replaced by gluconate. Control of the voltage-clamp protocol (*see* description of Fig. 1, below), collection of current data, and preliminary analysis were carried out via an EPC9 amplifier and Pulse software (HEKA Elektronik, Lambrecht, Germany), interfaced with a PowerMac G4 microcomputer (Apple Computer, Cupertino, CA). Most data were collected at 2 kHz and filtered at 250 Hz; exceptions are stated in the figure legends. For I-V analysis, currents were averaged over the last half of each trace, and the results transferred from Pulse software to Microsoft Excel, or to Wavemetrics Igor, for further processing.

The basic type of experiment underlying most of our reported data is shown in Fig. 1. Gigaseal formation was initiated by light suction of the patch pipette onto a visually "clean" area of yeast-cell membrane, and was monitored by a decline of current in response to a running 10-ms, 5-mV pulse. The membrane patch was then broken by a combination of suction and a brief high-voltage pulse (+750 mV, 100 μs). An interval of several minutes was allowed for equilibration between the cytoplasm and the pipette solution, then a reference voltage (holding voltage) of −40 mV was imposed. Thereafter, full scans of the membrane voltage (V_m) were generated via a staircase of 2.5-s pulses from +100 mV, +80 mV, ... to −200 mV in 20-mV decrements, with 0.5 s at the holding voltage between each pair of pulses. A compact, superimposed
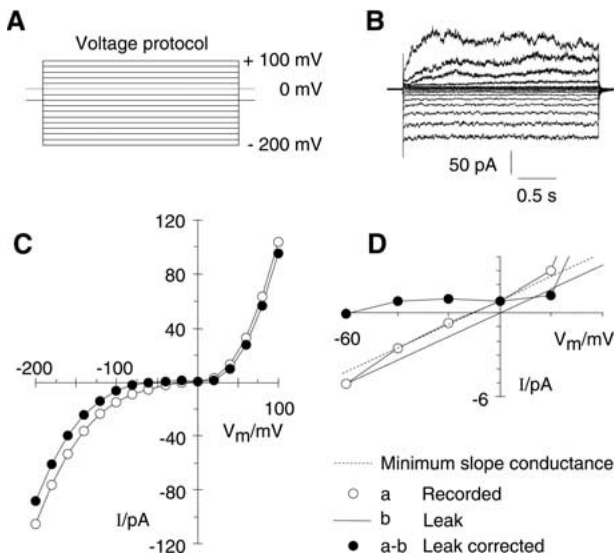
Fig. 1. Demonstration of the basic current-voltage experiment, and correction for the linear leak. (*A*) The voltage-clamp protocol for most experiments consisted of 2.5-s voltage-clamp steps at 20-mV intervals from + 100 mV to −200 mV, with all steps being taken from a holding voltage of −40 mV. Traces are shown superimposed. (*B*) Whole-cell transmembrane currents for the voltage steps of panel A from *S. cerevisiae* protoplasts, obtained with a patch electrode (Bertl et al., 1992, 1993, 1998): inward currents (plotted downward) are associated with the TRK proteins, outward currents (upward) are due to the yeast K⁺ channel Tok1p. (*C*) Steady-state current-voltage (*I-V*) relationship, with leakage correction. For each pulse, current was averaged over the interval 1.25 to 2.25 sec (from 50% to 90% of the trace length) and plotted against the clamped membrane voltage. Total leakage current through the patch-electrode seal and intact cell membrane was estimated as the ohmic current (least-squares fit) between 0 and −40 mV. The measured steady-state *I-V* relationship (*empty symbols*), from the traces in panel B, was corrected (*filled symbols*) by subtraction of the ohmic current. (*D*) Details of the correction procedure, shown on an expanded scale. Symbols as in panel C. *Dashed line*: regression line for the minimal slope of the experimental *I-V* curve. *Solid line*: ohmic leak, estimated from the slope of regression. Yeast strain EBC202 (*TRK1 TRK2 TOK1 pmr1Δ*). Buffer 5.5 (Table 2).

display of this voltage protocol is shown in Fig. 1*A*, and the corresponding membrane currents are shown in Fig. 1*B*. Downward, or negative, traces represent inwardly directed current (i.e., cations would flow into the cell, anions out of the cell) and reflect largely the behavior of the TRK proteins; upward, or positive, traces represent outwardly directed current (i.e., cations flowing out of the cell), and reflect largely the yeast potassium channel, Tok1p. The averaged steady-state current values in Fig. 1*B* have been plotted against the corresponding voltages from Fig. 1*A* and are shown in the current-voltage (*I-V*) plots of Figs. 1*C,D* (*empty circles*).

Leakage correction

Both the gigaseal and the cell membrane itself give rise to a small non-selective "leak"; and because the yeast cell and its physiological currents are also small, that leak can produce a significant fraction of the measured current. So an accurate picture of the physiological currents requires correction for the leak, but due to various unverifiable assumptions, there is no fully satisfactory way

to estimate that leak. Since our interest here is not in the whole yeast-cell membrane, but in the explicit properties of the TRK proteins, the best method of correction, in principle, would be to apply an inhibitor—one that is specific for the TRK proteins and that acts both rapidly and reversibly—to switch Trk1p and/or Trk2p on and off, and to calculate the resulting difference *I-V* curve, characterizing only what changes with the inhibitor, not the rest of the membrane nor the properties of the electrode seal. Unfortunately no such inhibitor exists, and an upper-bound correction for leakage current has been made by calculating the least-squares slope of the experimental *I-V* plot (*empty circles* in Fig. 1*C,D*) between 0 mV and −40 mV (*viz*. the dashed line drawn in Fig. 1*D*), and subtracting that conductance (*solid line* in Fig. 1*D*) from the experimental *I-V* plot to give the leak-corrected *I-V* curve (*filled circles* in Figs. 1*C,D*). This procedure arbitrarily sets the apparent membrane conductance to zero at the origin, but avoids glaring errors, such as unsupported negative conductances. (This computation sometimes yields a slight negative conductance, as between −20 mV and the origin in Fig. 1*C,D* but that is an artifact of data scatter around the least-squares fit.) The resulting corrected *I-V* plots usually show small positive currents at small negative voltages, and apparent reversal voltages (E_R) near the holding voltage of −40 mV. The significance of those values of E_R remains to be determined. Throughout this paper, data records are shown uncorrected for the ohmic leak, but the resultant *I-V* plots are shown corrected. The most important property of the corrected *I-V* curves for TRK proteins, especially in the presence of high cytoplasmic chloride, is the steep slope (large conductance) at voltages negative to −100 mV.

Because the large positive (upward) currents at positive V_m do not reflect behavior of TRK proteins, but of others, such as the K⁺ channel Tok1p, most of the current-voltage plots which follow have been truncated at slightly positive voltages.

Results

EXTRACELLULAR POTASSIUM IS IRRELEVANT TO THE LARGE TRK CURRENTS

Bihler et al. (1999) first reported the surprising result that changes of extracellular K⁺ concentration barely affect inward TRK currents through the *Saccharomyces* plasma membrane. That observation has now been confirmed and extended in two ways. First, as shown in Fig. 2, complete replacement of extracellular K⁺, whether by a neutral osmoticum such as sorbitol (panels *C*), or by a variety of alternative cations, including sodium (*data not shown*), choline (panels *A*) or N-methyl-D-glucamine (panels *B*) had no significant effect on the inward currents measured by patch-clamping, at any voltage. The data in Fig. 2 were obtained at extracellular pH = 5.5; but the same picture emerged at all other pH's tested: 7.5, 6.5, and 4.5, even though the voltage-dependence of inward currents was clearly shifted by changes of extracellular pH. In other words, removing extracellular K⁺ had, simply, no significant effect on the inward currents.

This result contrasted sharply with the effect of K⁺ removal on the outward currents mediated by Tok1p. That channel is known to close at extracellular K⁺ concentrations below ∼1 mM (Bertl &
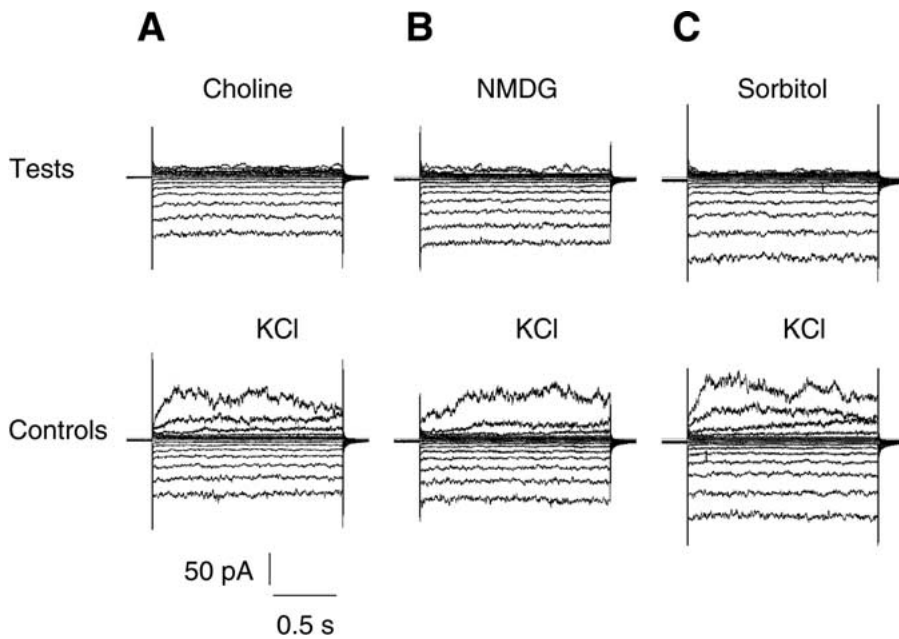
Fig. 2. TRK-dependent inward currents are independent of extracellular potassium. *Top row*: complete replacement of KCl in Buffer 5.5 by 150 mM choline chloride (*A*), NMDG (*B*, N-methyl-D-glucamine), or sorbitol (*C*). *Bottom row*: control measurements, after return to KCl-Buffer 5.5. 150-mM NMDG solution titrated to pH 5.5 with DMG (3,3-dimethyl glutaric acid). Yeast strain EBC202 (*TRK1 TRK2 TOK1 pmr1Δ*). Voltage protocol as in Fig. 1, except for the shorter pulse duration (1.5 s) and maximal voltage only to −180 mV. Each test represents at least four different cells.

Slayman, 1992; Ketchum et al., 1995; Vergani et al., 1997; Loukin & Saimi, 1999), and the near abolition of outward currents in the present experiments was taken to certify the effective removal of extracellular potassium. In fact, trace potassium in the perfusing solutions measured below 10 μM.

The second confirmation was that tests with a variety of potassium analogs, and with other cations often used as K^+-displacing or K^+-blocking ions, also had no effect on the inward currents. The full list of these ions is given in Table 3. The list includes, among others, cesium, tetraethylammonium, barium, and spermidine. (The variation of control measurements, between 58 pA and 124 pA, at −180 mV, reflects normal cell-to-cell variation, when spheroplasts are picked for their visually judged patchability, but without reference to cell size.)

PROTON BUFFER CAPACITY HAS NO EFFECT ON THE TRK CURRENTS

The previously reported strong dependence of TRK-mediated currents on extracellular pH (Bihler et al., 1999), defines a logarithmic relationship between current amplitude (at voltages negative to −100 mV), rather than a first-order linear dependence, which would be expected for simple proton currents or proton-coupled currents. It seemed possible, nevertheless, that protons might still carry the measured currents. But because these currents are large at the expected normal membrane voltage (−200 mV; $I_m \simeq$ 0.5 pA/μm^2 of cell surface) they should partially deplete the unstirred layer surrounding the cell of ions, such as H^+, which are present at micromolar or submicromolar concentrations (31.6 μM to 0.031 μM,

Table 3. TRK-dependent currents are not blocked by other alkali-metal ions, by K^+ transport inhibitors, or by polyvalent cations.

Cation name	Current at −180 mV (PA)	
	Control	+ 15 mM cation
Cs^+	−124.4	−113.5
Rb^+	−124.4	−125.7
Na^+	−104.0	−108.7
Li^+	−104.0	−113.1
TEA^+	−101.6	−101.0
TMA^+	−101.6	−106.0
Ba^{2+}	−101.6	−103.7
Zn^{2+}	−72.6	−70.6
Gd^{3+}	−90.8	−91.6
Spermidine^{3+}	−58.2	−58.5
Spermine^{4+}	−73.6	−59.2

Results have been corrected for the linear leak (*see* Fig. 1). Test cations were used as chloride salts, added to Buffer 4.5 (pH$_{out}$ = 4.5), except spermidine and spermine (Buffer 5.5). Control values are averages of before and after each test, and all values are representative of measurements on three or more different spheroplasts for each condition. Differences between control currents reflect mainly cell size. Strain EBC202 (*TRK1 TRK2 TOK1 pmr1Δ*). TEA$^+$: tetraethyl ammonium ion; TMA$^+$: tetramethyl ammonium ion.

for pH 4.5–7.5). Any such diffusional limitation should be suppressed by buffer capacities in the millimolar range, and enhanced by buffer capacities in the micromolar range, as has been thoroughly discussed in relation to proton transfer through lipid bilayer membranes (Gutknecht & Tosteson, 1973; Walter et al., 1982; Gutknecht, 1992).

Experiments were therefore conducted to test the effect of lowered buffer capacity in the bath solution upon time courses of TRK-mediated currents.
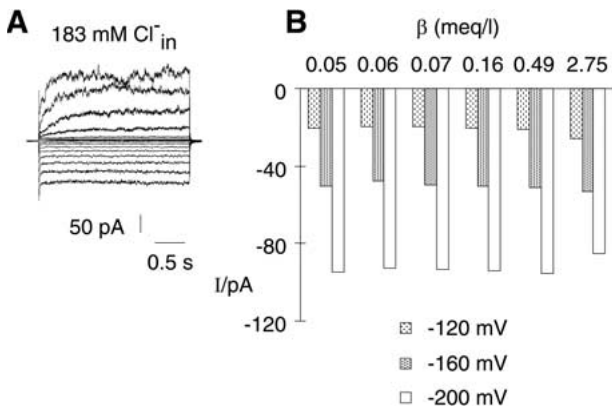
Fig. 3. TRK-dependent inward currents, at fixed pH_{out}, are insensitive to buffer capacity (β). (*A*) Whole-cell transmembrane currents of yeast protoplasts, with standard recording solutions (Table 2): Buffer G in pipette, Buffer 4.5 out (β = 0.49). (*B*) Summary of steady-state inward currents at three different clamped membrane voltages (−120 mV, −160 mV, −200 mV) from a single protoplast, representative of three. Measured buffer capacities shown along the abscissa, from 0.05 meq/L to 2.75 meq/L. All current tracings were flat, as in panel *A*, showing no tendency to relax. Modified Buffer 4.5, made with DMG at 0.0001 mM, 0.001, 0.01, 0.1, 1.0, & 10 mM, and titrated with HCl for the 3 lower concentrations or with Tris base for the three higher concentrations. Actual buffer capacities were measured by titrating the finished solutions with NaOH. Yeast strain EBC202 (*TRK1 TRK2 TOK1 pmr1* Δ).

Representative records are shown in Fig. 3*A*, and averaged results for all experiments (3 complete tests) are compared in Fig. 3*B*. Evidently, solution buffer capacity, in the range 0.05 to 2.75 meq.L⁻¹ .(pH unit)⁻¹ had no effect on the currents, a fact that was true at pH 5.5 and pH 6.0 as well (*data not shown*). Furthermore, none of the records, at any pH or buffer capacity, showed slow relaxations of current, which would be expected if the inward currents were depleting protons in the immediate pericellular space. These combined observations make it very unlikely that diffusion-limited proton movement, uncoupled from potassium, could carry the measured currents.

The necessary conclusion, from the K⁺-replacement, K⁺-blocking, and pH experiments, is that the TRK proteins in yeast have a conspicuous functional mode that involves neither potassium ions nor protons, but that does admit large inward currents under conventional patch-clamp conditions. It is difficult to avoid the inference that anion efflux must underlie these currents.

THE TRK PROTEINS CONDUCT AN EFFLUX OF CHLORIDE IONS

Since the predominant anion in the pipette solution (Buffer G) was chloride, with > 95% due to the 175 mM KCl, the simplest test was to replace KCl with potassium sulfate. Although there initially were problems maintaining gigaseals with sulfate-substituted Buffer G, even preliminary experiments showed a near abolition of the TRK-dependent currents. Eventual stable recording made the case unequivocal, as is illustrated in Fig. 4 (*left column, 2nd panel*, cf. *right panel*), and also emphasized that the switch between chloride and sulfate in the pipette had no major effect on yeast membranes generally, since outward currents due to the TOK1 channel did not change.

A variety of other anions also proved to be non-conducted replacements for chloride. These included gluconate, isethionate, and acetate (represented in Fig. 4), and MES, selenate, and phosphate (pH 7.0, so ∼40% monobasic, ∼60% dibasic), all detailed in Table 4, middle column. Gluconate was the most satisfactory, in giving stable and clean records, and became the cytoplasmic "reference" ion of choice. Partial replacement of the pipette KCl with K-gluconate left appropriately reduced currents, as demonstrated in the middle panel of Fig. 4 (96 mM Cl⁻).

Further experiments searched for possible inhibitory effects of these and other anions on the Cl⁻-dependent inward currents. These results are summarized in Table 4, right column, for tests made mostly with 30–40 mM test anion replacing equivalent chloride in Buffer G. By the criterion of reducing the chloride-dependent currents, many of the tested anions appeared to be inhibitory, but very weakly so, diminishing the currents only slightly more than expected for simple chloride removal. Glutarate had no significant effect, and the well-known anion-channel blockers, DIDS and NPPB (at 0.1 and 1.0 mM) had no effect. Thus, while the TRK proteins do conduct chloride ions and other halides (*data not shown*), the pathway involved was not susceptible to conventional Cl⁻-channel blockade, even though it discriminates very well against non-halide anions.

VARIATION OF TRK CURRENTS WITH *TRK1*- OR *TRK2*-GENE EXPRESSION AND WITH STRAIN BACKGROUND

The original patch-clamp experiments on the yeast TRK proteins (Bihler et al., 1999) and a recent and more detailed study on a full range of deletion strains for *TRK1*, *TRK2*, and *TOK1* (the yeast K⁺-channel gene; Bertl et al., 2003), identified currents through Trk2p, but not through Trk1p. However, the amplitude of observed currents varied considerably from strain to strain and from time to time (1997–1998 *vs.* 2002–2003), in a way to suggest that strain background has a major influence on the observations. We have therefore undertaken a detailed comparison of several sets of strains, particularly from the W303 and S288c backgrounds, in order to develop data from experiments that are as nearly homogeneous as possible: *viz.*, cells grown, spheroplasted, and measured under virtually identical conditions, and selected
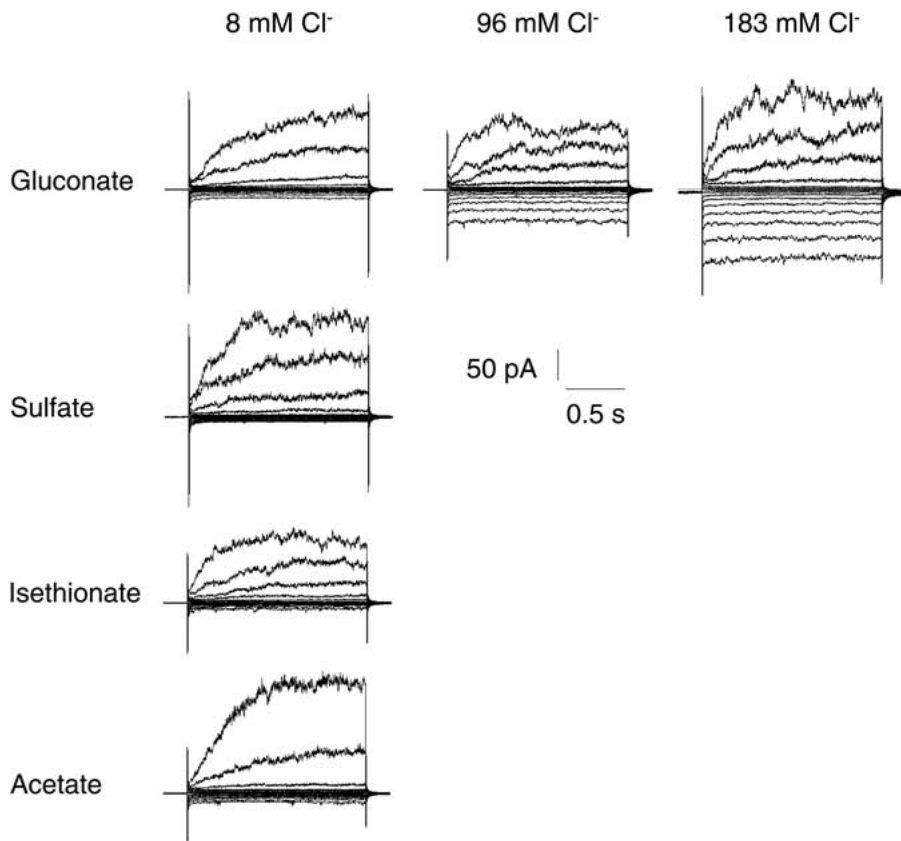
Fig. 4. TRK-dependent inward currents depend on the intracellular anion. *First column:* Isosmotic replacement of the normal 175 mM KCl in Buffer G (pipette solution, intracellular) by K-gluconate, K$_2$SO$_4$ (117 mM), K-isethionate, or K-acetate. Note very small residual inward (downward) currents in all cases. *Top row:* Full, half, or no replacement of pipette KCl with K-gluconate. Right panel is the normal control. Note approximate doubling of inward currents from half replacement, to the control. Extracellular solution was Buffer 5.5 in all cases. Yeast strain EBC202 (*TRK1 TRK2 TOK1 pmr1Δ*). Standard whole-cell patch-clamp recordings, with voltage protocol as in Fig. 1, but clamp pulses only to −180 mV. Pulse duration, 1.5 sec. Each record set is representative of 3–4 replicates on different spheroplasts.

for the same size and microscopic appearance: ∼8 μM diameter for both BS202 (W303 background) and PLY232 (S288c).

Summary records from these experiments are displayed in Fig. 5. In all cases, the inward currents remaining after deletion of *TRK2* were slightly larger than those remaining after deletion of *TRK1* (*cf.* Fig. 5 line *1* with line *2*, for each background), implying that in wild-type spheroplasts Trk1p is responsible for somewhat more than half of the total inward current. Considering all of the available data, 50–70% of the inward currents of wild-type cells persisted upon removal of Trk2p, whereas 30–50% persisted after removal of Trk1p. Obvious variations were small compared with the total currents, however, and the simplest inference is that roughly 50% of the current in wild-type cells is related to each of the two proteins, regardless of strain and background. The third row in Fig. 5, with records from doubly deleted strains (*trk1Δ trk2Δ*), certifies that only very small inward currents remained in the complete absence of TRK proteins, as had also been reported previously (Bihler et al., 1999; Bertl et al., 2003).

The influence of strain background, illustrated in Fig. 5 (*cf.* column *B* with columns *A* and *C*) is demonstrated quantitatively in Fig. 6, displaying the individual and averaged current-voltage curves from all experiments on the three wild-type strains: BS202, PLY232, and EBC202 (W303, *pmr1Δ*; records not shown in Fig. 5). Roughly speaking, the currents at corresponding voltages were twice as large in BS202 (panel *A*) as in PLY232 (panel *B*), and were nearly twice as large again in EBC202 (panel *C*), where the background effect was augmented by deletion of *PMR1*. Most of the latter effect can be attributed to the almost unavoidable selection of larger spheroplasts for patch recording in *pmr1Δ* strains (*viz.*, ∼10 μM diameter rather than 8 μM). The relative contributions of Trk1p and Trk2p to the inward currents were stable and rather independent of strain background, as demonstrated in Fig. 7, panels *A* and *B*. Furthermore, the summed average currents were approximately the same amplitude as the averaged wild-type currents from the experiment of Fig. 6 (especially panel *3D*), and could be very nearly superimposed on those currents, as shown in Fig. 7*C* (dashed curves). Thus, when patch-clamp measurements were made under carefully controlled conditions, with cells of equivalent size selected, then the two TRK proteins contributed equally to the total inward membrane current, roughly but not exactly judged.

The high-affinity K$^+$ transporter Trk1p has been found essential for growth of yeast on K$^+$ concentrations below 1 mM (Gaber et al., 1986; Ko, Buckley & Gaber, 1991; Haro & Rodriguez-Navarro, 2002), and that protein/gene is assumed to be upregulated during

Table 4. Intracellular anions that neither support nor block the TRK-dependent inward currents

Anion in the pipette	Current at −180 mV (pA)	
	Chloride full replacement	Blocking test (Anion 30–40 mM)
Cl$^-$ (Control)	−102.0 ± 15.5	−
Gluconate$^-$	−11.1	−57.3
SO$_4^{2-}$	−7.9	−72.7
SeO$_4^{2-}$	−9.5	nt
HCO$_3^-$	−3.2	nt
H$_2$PO$_4^-$	−1.2	nt
BrO$_3^-$	nt	−51.1
Azide	nt	−87.4
Isethionate	+4.6	nt
Formate	−15.9	−76.4
Acetate	−4.4	−44.3
Monochloroacetate	nt	−45.4
Trichloroacetate	−8.0	−41.7
Glutarate	nt	−92.5
Polyaspartate	nt	−111.1
MES	−18.6	nt
Sorbitol	−2.6	nt
DIDS	nt	−107.0
NPPB	nt	−129.2

All values have been corrected for the linear leak (*see* Fig. 1). *nt* = not tested.

Blocking tests for most anions replaced 30 mM Cl$^-$ by 30 mM of test anion ([Cl$^-$]$_{in}$ = 153 mM), except for the following:
a) Gluconate: 44 mM, + 139 mM Cl$^-_{in}$
b) Sulfate: 44 mM, + 140 mM Cl$^-_{in}$
c) Azide: 3 mM, + 180 mM Cl$^-_{in}$
d) Acetate: 87.5 mM, + 95 mM Cl$^-_{in}$
e) Trichloroacetate: 87.5 mM, + 95 mM Cl$^-_{in}$

Full-replacement tests usually used the osmotically equivalent concentration of K$^+$-salt of the test anion, instead of the normal 175 mM KCl, and were carried out at pH 5.5.
Exceptions:
a) Selenate: pH4.5; also, current measured at −160 mV.
b) HCO$_3^-$: 91 mM, bubbled with 40% CO$_2$, pH 7.04; + 84 mM K-gluconate + 8 mM Cl$^-_{in}$.
Data from whole-cell patch recordings, representative of measurements on 3–5 different cells for each condition.
Strain EBC202 (*TRK1 TRK2 TOK1 pmr1Δ*).
DIDS (4,4′-diisothiocyanatostilbene-2,2′-disulfonic acid), NPPB (5-nitro-2-(3-phenylpropyl-amino) benzoic acid, and polyaspartate [poly-(α,β)-DL-aspartic acid, sodium salt (M$_r$ = 2,000–10,000)] were added to Buffer G at 0.1 mM, 0.1 mM, and 0.1% (w/v), respectively.

potassium starvation. Vidal et al. (1990), however, discovered a suppressor of weak K$^+$ uptake in *trk1Δ* strains, which proved to be a promoter mutation in the *TRK2* gene, such that *TRK2* messenger expression was upregulated by about 10-fold. The resultant inward currents in such a strain from the S288c background are shown in Fig. 5, panel *D2*, to be compared with those in panel *B2*. The ratio of 5- to 6-fold is in reasonable agreement with expectation on the basis of the change in messenger concentration. It is therefore clear that the TRK2 protein can support very large inward currents when its biosynthesis is upregulated.

FUNCTIONAL SIGNIFICANCE OF THE STRAIN DIFFERENCES

Functional variations due to strain background differences are a well-known, though ill-documented, phenomenon in yeast biology. By direct resequencing of the *TRK1* and *TRK2* genes and their long 5′ and 3′ flanks (*data not shown*), we demonstrated the absence of any significant difference within the gene/protein sequences themselves, between BS202 and the Yeast Genome Database, which represents S288c. That result was expected, and a further search must be made for the source of difference between W303-derived and S288c-derived TRK currents. A simpler question, however, was whether the difference might have any functional significance, or whether it might be related to any potassium-affected growth differences between the two backgrounds. Quantitative growth experiments were conducted in microtiter plates (*see* Materials and Methods) to test this question. At low pH (4.5) there were no growth differences. At pH 7.5 the kinetics of growth was slightly different for the two strain backgrounds: W303-derived strains grew slightly faster in exponential phase (doubling times shortened by 10–20 min), but they approached the stationary state more slowly than did the S288c-derived strains (*data not shown*). Even those differences were independent of external potassium concentration, from 0.05 mM to 10 mM, and nearly independent of the presence or absence of Trk1p or Trk2p, and so are unlikely to be related to currents through the TRK proteins.

POTASSIUM CURRENTS IN LOW-CHLORIDE CELLS

Since there is little doubt that the primary function of the yeast TRK proteins is potassium accumulation, it follows that the currents induced by artificially elevated cytoplasmic chloride must represent a secondary function: perhaps the steady-state ejection of chloride—even into high chloride solutions (driven by a normal V_m near −200 mV)—or perhaps an unknown emergency function. It also seemed likely that removal of "excess" intracellular chloride might reveal bona fide potassium transport currents related to the TRK proteins. That did, in fact, prove to be the case, and results from two series of experiments are demonstrated in Fig. 8. Cytosolic (pipette) chloride was fixed at 1.2 mM, and, as in the experiments of Fig. 4, considerable patience was needed to overcome instability in the gigaseals. After 10–15 min, however, recordings usually settled down and small K$^+$-dependent inward currents could be observed. Comparison of records from a strain expressing both TRK genes (Fig. 8, *left column*, strain EBC202) with records from a strain deleted of both genes (Fig. 8, *right column*, strain EBK202) revealed inward currents of 4–5 pA, at −200 mV, in response to 50 μM extracellular K$^+$, and currents up to 20 pA at
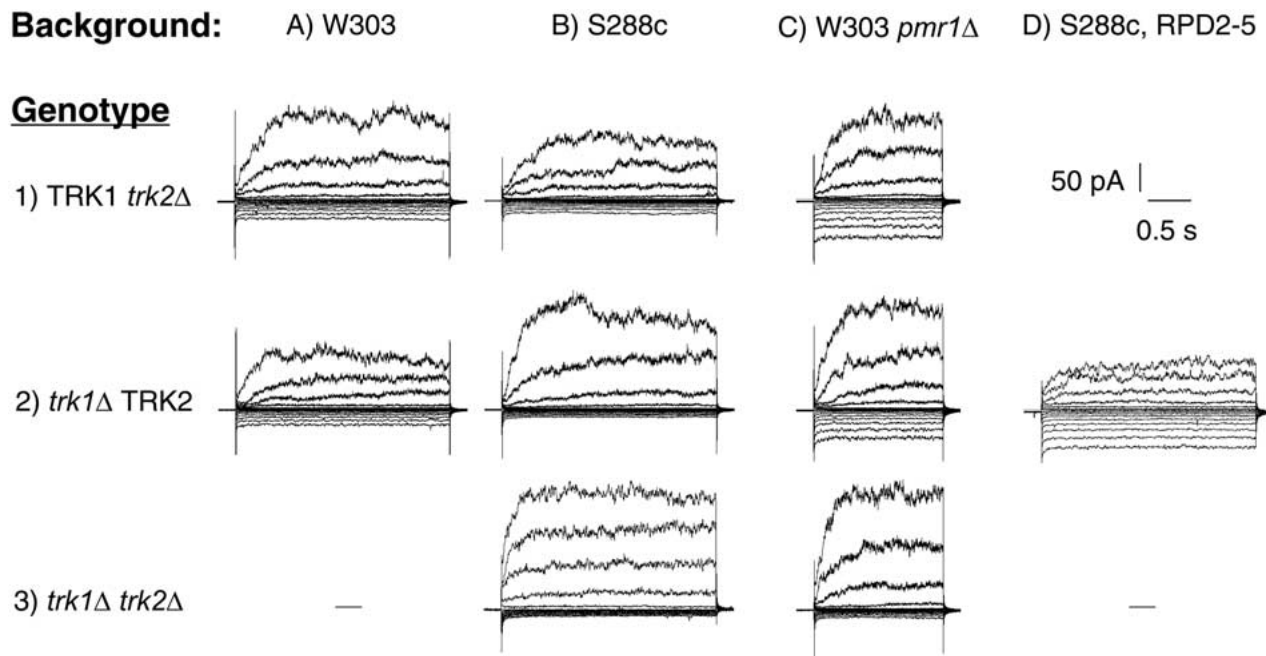
Fig. 5. Both Trk1p and Trk2p contribute measurable inward currents, regardless of strain background. Significant inward (downward) currents remained whenever either wild-type gene, *TRK1* or *TRK2*, was present. Chosen record sets are representative for 4–8 trials on 2–6 protoplasts for each strain. Strain identification in each column, top to bottom: *Column A:* EBF202, EBE202. *Column B:* PLY236, PLY234, PLY240. *Column C:* EBJ202, EBH203, EBK202. *Column D:* AB541, with mutation upregulating the promoter for *TRK2* (Vidal et al., 1990). Note the greatly increased size of TRK2 currents with upregulation of that promoter (*cf.* panels *D2* and *B2*). Experimental conditions as in Fig. 1, except that (i) the voltage pulses were run only to −180 mV in these tests, instead of to −200 mV; (ii) in tests with the *pmr1*Δ strains (column *C*), the pulse duration was 1.5 s. instead of 2.5 s; and (iii) the record sets *B3* and *D2* were collected at 1 kHz and filtered at 100 Hz, instead of the usual 2 kHz and 250 Hz.

−200 mV, in the TRK wild-type strain (EBC202), responding to 150 mM extracellular K⁺. Similar results (*not shown*) were obtained with pipette chloride ($[Cl^-]_{in}$) at 0.1 mM, instead of 1.2 mM.

Quantitative comparison of the two sets of records in Fig. 8 is facilitated by the steady-state current-voltage plots in Fig. 9: panel *A* corresponding to data from the left column of Fig. 8, and panel *B* corresponding to data from the right column of Fig. 8. In the absence of the two TRK proteins, there were small residual outward currents at membrane voltages positive to about −200 mV for the lower values of $[K^+]_{out}$, and positive to about −90 mV for $[K^+]_{out} = 150$ mM. Intracellular $[K^+]$ was kept at 30 mM by the pipette solution in these experiments, so the calculated reversal voltages for K⁺ in the four cases were approximately −160 mV, −85, −28, and +40 mV, respectively, meaning that K⁺ currents would be inward, not outward. The origin of these residual currents is not yet known[1], but their linearity in *trk1*Δ *trk2*Δ cells implies that simple difference *I-V* curves, obtained by subtracting the linear currents

(offset plus leak) would yield the clearest description of TRK currents. The resulting corrected plots are shown in Fig. 9*C*. The outward currents (upward, to the right of the ordinate, truncated at +60 mV) are related to the behavior of the TOK1 channel, and only the inward currents (downward, to the left of the ordinate) represent the TRK-mediated K⁺ fluxes.

An Eadie-Hofstee plot of the leak-corrected conductances, calculated over the interval −200 mV to −160 mV, is shown in Fig. 9*D*. The smooth curve is a least-squares fit for the sum of two Michaelis functions, with best-fit $K_{0.5}$ values of 46 μM and 6.8 mM extracellular K⁺, comfortably close to the values (∼30 μM and ∼10 mM) expected from flux data in the literature for Trk1p and Trk2p (Armstrong & Rothstein, 1964; Rodriguez-Navarro & Ramos, 1984; Ramos et al., 1994). The corresponding V_{max} values of 59.4 pS and 123 pS reflect the relative maximal contributions of Trk1p and Trk2p to K⁺ influx in low-K⁺ cells having normal membrane voltages (*viz.*, near −200 mV). Corresponding inward currents at −200 mV, for saturating $[K^+]_{out}$, would be 4.1 pA/cell and 8.6 pA/cell; for the 10-μm-diameter cells (*pmr1*Δ) used in the experiment of Fig. 8, these currents imply net K⁺ influxes of 4.9 mM/min and 10.2 mM/min, via Trk1p and Trk2, respectively. The

---

[1] In addition to the seal conductance, the curves in Fig. 9*B* contain currents due to other transporters in the yeast membrane, and possibly also small offsets due to liquid junctions between pipette and bath solutions.
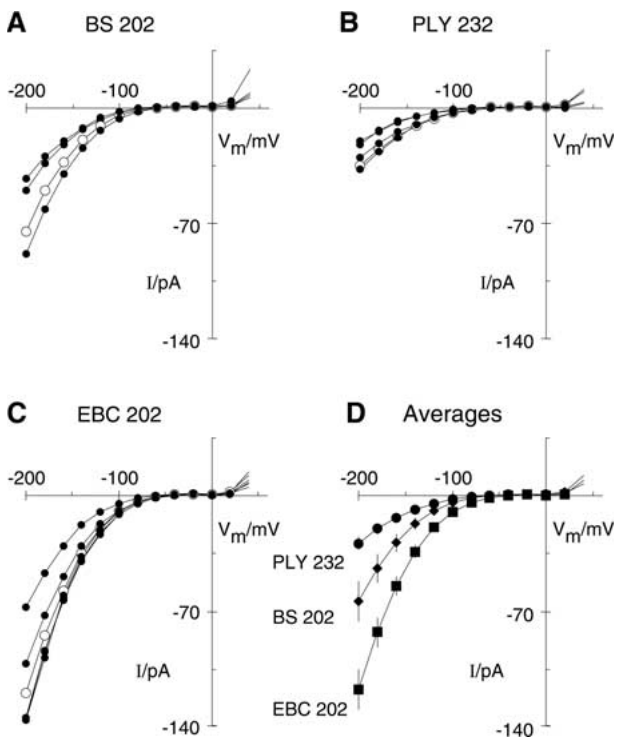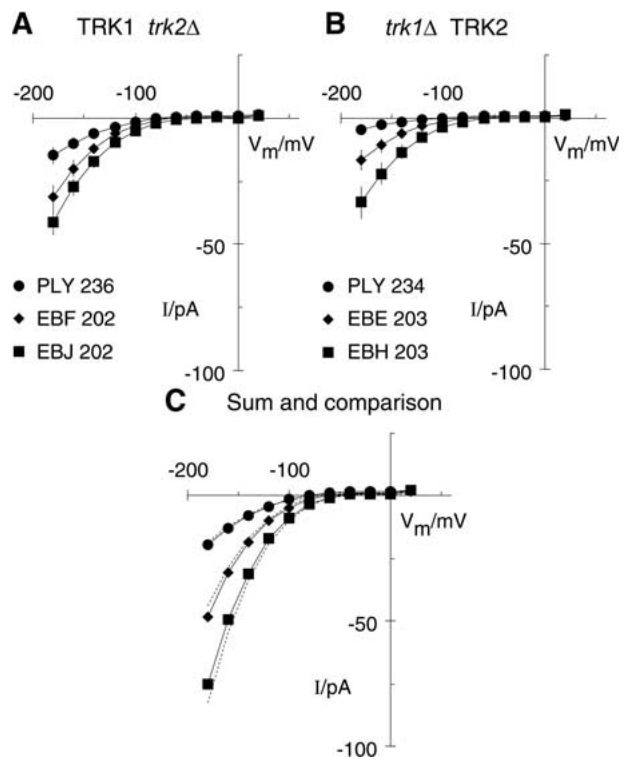
Fig. 6. Spread of measured TRK currents is narrow, in any one strain and genetic background, for homogeneous experiments. Current-voltage relationships from all trials on strain BS202 (*A*; *n* = 4), on PLY232 (*B*; *n* = 5), and on EBC202 (*C*; *n* = 6). Panel *D* shows the averaged *I-V* plots for all three strains; error bars, ± 1 SEM at each voltage. Spheroplasts were selected as nearly as possible the same size: ∼8 μm diameter for BS202 and PLY232; ∼10 μm diameter for EBC202. Buffer 5.5. Open symbols used only for clearer definition of individual I-V curves.

Fig. 7. Trk1p-currents + Trk2p-currents = wild-type currents. Class averages for all trials as in Fig. 5. (*A*) Average currents via Trk1p (Trk2p deleted), in each of the three backgrounds. (*B*) Average currents via Trk2p (Trk1p deleted), in each of the three backgrounds. (*C*) Sum of averaged Trk1p- and Trk2p-currents from panels *A* and *B* (*plotted points, solid curves*), compared with wild-type currents from Fig. 6*D*, above (*dashed curves*). Averages are plotted to −180 mV, because voltage scans for some curves in each set, related to Fig. 5, reached only to −180 mV, instead of the usual −200 mV.

overall numbers are compatible both with the reported maximal velocities of chemically measured transport, and with expectation based on the likely current density delivered by the proton pump (*see* Introduction).

Although the calculations above are based on a small number of experiments—hence the actual numbers should not yet be regarded as firm—the overall results describe the two potassium uptake systems in long-familiar terms: Trk1p is a high-affinity, low-velocity system that runs fast enough —and from low enough extracellular concentrations—to handle the uptake required by growth under most conditions. It thus appears as the essential system. Trk2p, on the other hand, is a low-affinity, high velocity system, which is not able to scavenge K⁺ from rarefied environments, but is able to restore depleted cells more quickly when potassium becomes plentiful.

Finally, it is evident by comparison of Fig. 8 with Fig. 2 that this potassium sensitivity of the TRK proteins emerged only when intracellular chloride was brought to a physiologically reasonable

range, near or below 1 mM. This almost certainly means that elevated cytosolic chloride not only commandeers its own pathway through the TRK proteins, but also deactivates the normal pathway(s) for potassium.

Discussion

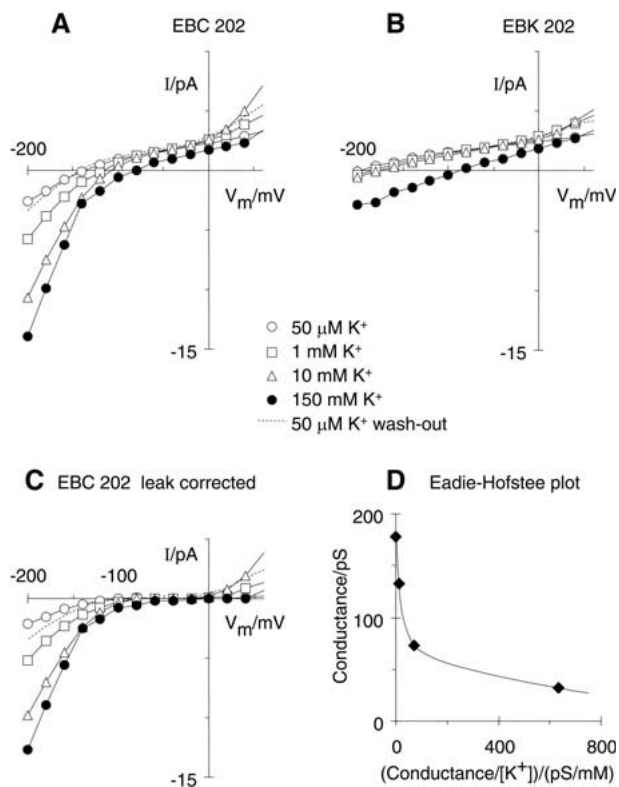### INFERENCES FROM CHLORIDE CONDUCTION VIA TRK PROTEINS

TRK-dependent currents, observed under the "normal" patch-clamp conditions for yeast spheroplasts, typically measured ∼100 pA (background-dependent) at −200 mV: five- to 10-fold larger than had been expected for active transport of potassium at the normal resting membrane voltage. Given the size of most yeast cells assayed in these experiments (∼8 μm diameter, 200 μm² of surface area), the amplitude of currents also strains the limits of plausibility for carrier-mediated transport generally, at reasonable
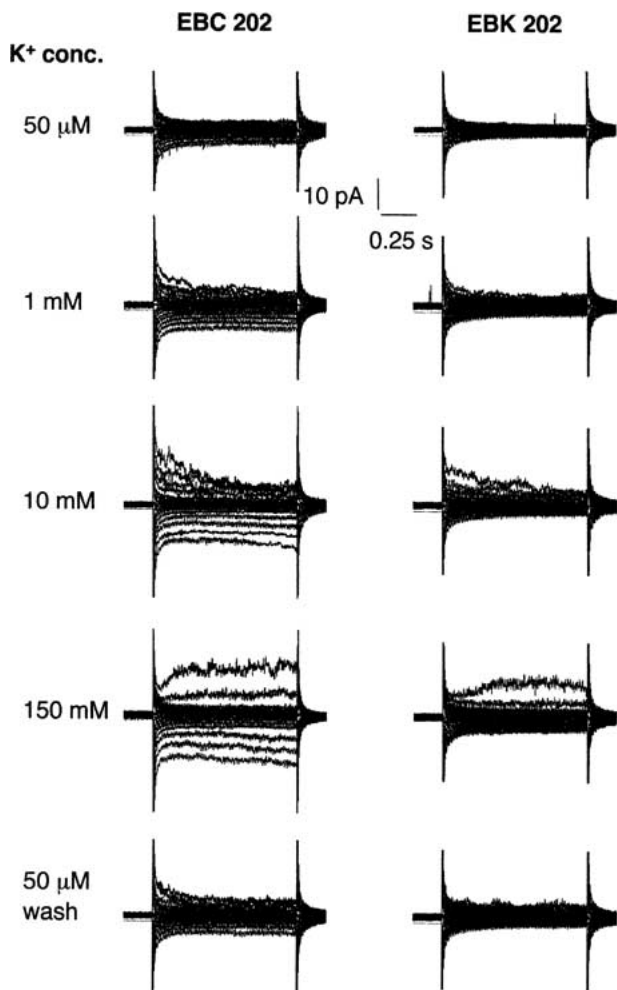
Fig. 8. Residual inward currents, with low intracellular chloride, are potassium-dependent. *Left column*: Representative record sets from strain EBC202 (*TRK1 TRK TOK1 pmr1Δ*) spheroplasts at different $[K^+]_{out}$: 50 μM to 150 mM. *Right column*: Control recordings from strain EBK202 (*trk1Δ trk2Δ TOK1 pmr1Δ*), deleted of both TRK genes. Data are representative of 3–5 different spheroplasts for each condition. Precautions taken to keep $[K^+]_{in}$ low (*see* Materials and Methods for details) included 12-h K^+ starvation before spheroplasting, reduction of $[K^+]$ in sealing buffer to 50 μM, reduction of $[K^+]$ and $[Cl^-]$ in the pipette (intracellular) solution to 30 mM and ~1.2 mM. respectively, and much shortened pulse durations: 1 s instead of 2.5 s.

Fig. 9. Current-voltage analysis of the K^+-dependent TRK currents reveals two distinct components, compatible with the known K^+-transport properties of Trk1p and Trk2p. (*A*) Steady-state *I-V* plots for spheroplast expressing both wild-type TRK proteins (strain EBC202, left column of Fig. 8). (*B*) Corresponding plots for cell lacking both TRK proteins (strain EBK202, right column of Fig. 8), showing small but significant TRK-independent linear currents at negative voltages. These plots indicate that linear components of current in panel *A* are unrelated to the TRK proteins. (*C*) Difference *I-V* plots from panel *A*, corrected by subtracting the linear-current component of each curve, viz., the leak *plus* the offset, (*D*) Eadie-Hofstee plot of the slope conductances, between −160 mV and −200 mV, in panel *C*. Fitted parameters for the two kinetic components of TRK-dependent current are V_{max} (limiting conductances) = 59.4 pS & 123 pS; and $K_{0.5}$ = 46 μM & 6.8 mM ($[K^+]_{out}$), respectively.

carrier densities in the membrane (~1000 sites/μm²). It is likely, therefore, that chloride ions traverse the TRK proteins by a process of constrained diffusion similar to channel-mediated transport. Our inability, in several attempts, to demonstrate a suitable reversal voltage for chloride-dependent currents presumably had two causes: a very rapid collapse of steady-state currents at pulse end (too brief tail currents), and a very negative activation voltage (ca. −200 mV) relative to the practicable values of E_{Cl} (positive to approximately −40 mV).

Chloride movements through the TRK proteins, then, may be akin to the widely observed "chloride-

channel" behavior of mammalian amino-acid and neurotransmitter transporters (Lester, Cao & Mager, 1996; Lin, Lester & Mager 1996; Arriza et al., 1997). This phenomenon has been studied mainly after expression of the cloned transporters in *Xenopus* oocytes, whose cytoplasm is uncommonly rich in chloride (Weber, 1999); and the phenomenon disappears after oocytes have been dialyzed to remove the cytoplasmic Cl^- (Arriza et al, 1997; work on EAAT5). That disappearance has a profound effect on the shape of the overall current-voltage curves of the transporters, which convert from weakly inward-rectifying (concave downward over the voltage range −20 to −120 mV) to ohmic or weakly outward-rectifying. Preliminary *I-V* analysis of yeast Trk2p, expressed in *Xenopus* oocytes (G. Zeng and C.L.

Slayman, unpublished experiments) also shows a weak inward rectification, and similar reports have been published on plant homologs of Trk2p, *viz.* *Triticum* (wheat) and *Arabidopsis* HKT1 proteins (Gassmann, Rubio & Schroeder, 1996; Liu et al., 2000; Uozumi et al., 2000; Horie et al., 2001; Mäser et al., 2002). The potential complication of chloride conductance with these transporters would be interesting to investigate.

The yeast TRK proteins themselves may also provide a model for chloride conduction through the neurotransmitter transporters. In this regard, it is especially interesting that present folding models of the glutamate transporters (Wadiche, Amara & Kavanaugh, 1995; Arriza et al., 1997) contain at least two "P-loop"-like structures and one very long hydrophilic loop placed, at current reading, extracellularly, between the 3rd and 4th transmembrane helices, similar to the original model for TRK proteins, i.e., prior to the K^+-channel-like model of Durell & Guy (1999), which has been experimentally confirmed by Kato et al. (2002) and Zeng, Pypaert & Slayman (2004). There is a significant difference, however, between chloride permeation through the neurotransmitter transporters and the TRK proteins: in the former, the chloride currents are activated by the normal substrates (e.g., glutamate $+ Na^+$, for EAAT5; Arriza et al., 1997), whereas in the TRK proteins, high cytoplasmic chloride elicits chloride currents in the absence of extracellular substrate (K^+; Fig. 2) and also seems to preclude the normal transport of that substrate (*cf.* Figs. 4, 8 above).

The actual mechanism by which chloride traverses these proteins, either the yeast TRK proteins or the mammalian amino-acid and neurotransmitter transporters, remains to be determined. With the customary high-level expression of membrane proteins in oocytes, recording of currents is easy, and current traces are smooth, without analyzable noise from which true channel-like behavior might be deduced. The term chloride "channel" is therefore used with these proteins in a very loose or generic sense, rather than a specific sense. Current tracings from yeast cells, with ~0.01% of the surface area of a typical oocyte, do display appreciable noise, evident in most of the records of Figs. 1–5. For technical reasons, this noise has not yet been analyzed for channel-like components, but qualitative comparison of it with the almost-simultaneously recorded noise of the outward rectifier is revealing. The bona fide potassium channel, Tok1p, displays both high-frequency and low-frequency gating, has an open-channel conductance of ~40 pS, and is present at a density of about $1/\mu m^2$ of membrane surface (Bertl & Slayman, 1992; Bertl et al., 1993). The resulting noise on the outward (upward) traces is both much larger and much more shaped by low-frequency components than is the noise on the inward traces, for

equivalent steps of voltage. This comparison implies that the chloride-dependent currents through TRK proteins are mediated by small, high-frequency "gating" events. Even the "normal" K^+-transport process in the TRK proteins may be characterized by such events, since Bossemeyer et al. (1989) have argued that the TrkH,G system of *E. coli* has an unusually high turnover number for a carrier system: 10^4–10^5 ions.site⁻¹.s⁻¹.

Considerable evidence is now emerging for bona fide channel-like transit of ions through membrane carrier proteins, under special conditions (*see* e.g., Arriza, 1997; Artigas & Gadsby, 2003; Kettner et al., 2003), and such conductance can arise, in a whole-cell membrane, either as sporadic events affecting a few molecules with large conductance, or as common events affecting many molecules with small conductance. Chloride conduction through the yeast TRK proteins would conform to the latter alternative.

POTENTIAL FUNCTIONS OF TRK-DEPENDENT CHLORIDE CURRENTS

Although no one has taken care to scrub *Saccharomyces* growth media of chloride, down to namomolar concentrations, chloride need not be added deliberately to media in order to produce rapid growth. This means that chloride can be only a trace element in the growth of yeast. Chloride uptake by yeast has been observed as a sluggish process, compared with that, e.g., for phosphate and potassium (Coury et al., 1999); but recently, intracellular chloride was demonstrated to be sustained in the range of 0.1–0.2 mM, at extracellular concentrations below 10 μM. Yeast can thus maintain Cl⁻ concentration ratios of 10–100, against a membrane voltage that should drive anions toward a reversed ratio greater than 1000. This concentrating ability has now been attributed to the protein/gene YHL008c, a homolog of bacterial nitrate-formate transporters (Jennings & Cui, 2003). The presence of such machinery, along with a bona fide chloride channel (Gef1p; Greene et al., 1993; Huang, Chuat & Galibert, 1994) localized in intracellular membranes (Schwappach et al., 1998), indicates that intracellular chloride does play a significant role in yeast metabolism, despite its trace nature. Several such roles have been suggested: as a mobile ion for charge balance during vesicular acidification by H^+-ATPases (Wada et al., 1992), and as a co-factor in the activation of critical enzymes, especially aminopeptidase I (Röhm, 1985) and the multi-copper oxidase Fet3p, which is involved in iron transport (Davis-Kaplan et al., 1998; Gaxiola et al., 1998). Other, as yet undescribed, roles for cytosolic chloride probably also exist in yeast, since a considerable variety of enzymes have been described as chloride-dependent in other cellular systems (*see* e.g., Günther et al., 1998; Aghajari et al., 2002).

One likely role, then, for voltage-driven chloride efflux through the TRK proteins would be to balance the chloride influx system in yeast. Maximal influxes measured by Jennings and Cui (2003) approximate 0.1 fMoles/min per cell (*personal communication*), and effluxes estimated from quantitative analysis of the inward currents (Kuroda et al., *unpublished observations*), over the range 0.01–8 mM, are in the same range. Still, it seems unlikely that this peculiar property of the TRK proteins, or especially of the mammalian neurotransmitter transporters, would have evolved for the sole purpose of exiting chloride. For yeast and other fungi that have very acidic metabolisms, escape of metabolic acid anions would be a more plausible role for generalized anion permeability. The most obvious such anion is bicarbonate, which has been tested (Table 4) and found neither to mimic, nor to inhibit, the chloride currents. Krebs' cycle anions and amino acids remain to be tested.

Circumstances that raise intracellular chloride significantly beyond 10 mM, however, should have profound effects upon the metabolism of yeast and of any other organisms with similarly sensitive TRK transporters. This is due to the fact that large chloride-dependent currents must be strongly depolarizing in the absence of voltage-clamping. The related ascomycete *Neurospora crassa* is, in fact, one such organism whose chloride sensitivity was tested during the measurement of spherocyte characteristics with penetrating microelectrodes (Blatt & Slayman, 1983; Rodriguez-Navarro et al., 1986). Conventional salt-filled electrodes with chloride concentrations above 500 mM produced rapid membrane depolarization, such that it was difficult to estimate the normal or "resting" membrane voltage even as a transient, following impalement. The collapse of membrane resistance and rise of cytosolic chloride concentration went in parallel. Certification of this result after expression of the *Neurospora TRK1* gene in a yeast strain deleted of both native TRK genes would be a very useful exercise, as would similar testing of the plant and bacterial TRK homologs expressed in yeast.

A Role for Chloride in Salt Tolerance?

A major requirement in practical, agricultural plant science, as well as in the basic sciences of plant and microbial membrane functions, is to understand the complex processes involved in tolerance, or intolerance, to elevated concentrations of ordinary salt. However, despite the fact that chloride-ion concentrations are similar to sodium-ion concentrations in most environments, the overwhelming emphasis of transport and metabolic studies has been upon sodium ions. Perhaps that is because sodium channels

and transporters are more familiar features of cell membranes than are chloride-transferring systems. Or perhaps it is because chloride is generally at much lower intracellular concentrations than sodium (or potassium), being replaced as counterions by proteins, bicarbonate, phosphate, or a variety of metabolic acid anions. Whatever the case, the fact that elevated cytosolic chloride concentrations can drastically change the functional properties of some TRK proteins, at least in fungi and perhaps plants, and the properties of certain amino-acid and neurotransmitter transporters in mammalian systems, raises two large questions for future investigation: 1) What other membrane proteins are susceptible to chloride in this fashion? 2) To what extent does conventional salt intolerance, especially in crop plants, reflect chloride toxicity, rather than only sodium toxicity?

References

Aghajari, N., Feller, G., Gerday, C., Haser, R. 2002. Structural basis of α-amylase activation by chloride. *Protein Sci.* **11:**1435–1441

Anderson, J.A., Huprikar, S.S., Kochian, L.V., Lucas, W.J., Gaber, R.F. 1992. Functional expression of a probable *Arabidopsis thaliana* potassium channel in *Saccharomyces cerevisiae*. *Proc. Natl. Acad. Sci. USA.* **89:**3736–3740

Armstrong, W.McD., Rothstein, A. 1964. Discrimination between alkali metal cations by yeast. I. Effect of pH on uptake. *J. Gen. Physiol.* **48:**61–71

Armstrong, W.McD., Rothstein, A. 1967. Discrimination between alkali metal cations by yeast. II. Cation interactions in transport. *J. Gen. Physiol.* **50:**967–988

Arriza, J.L., Ellasof, S., Kavanaugh, M.P., Amara, S.G. 1997. Excitatory amino acid transporter 5, a retinal glutamate transporter coupled to a chloride conductance. *Proc. Natl. Acad. Sci. USA.* **94:**4155–4160

Artigas P., Gadsby, D.C. 2003. Na$^+$/K$^+$-pump ligands modulate gating of palytoxin-induced ion channels. *Proc. Natl. Acad. Sci. USA.* **100:**501–505

Bakker, E. 1993a. Cell K$^+$ and K$^+$ transport systems in prokaryotes. *In:* Bakker, E.P., (ed) Alkali Cation Transport Systems in Prokaryotes. pp 205–224, CRC Press, Boca Raton, FL

Bakker, E. 1993b. Low-affinity K$^+$ uptake systems. *In:* Bakker, E.P., (ed) Alkali Cation Transport Systems in Prokaryotes. pp 254–276, CRC Press, Boca Raton, FL

Bañuelos, A.A., Klein, R.D., Alexander-Bowman, S.J., Rodriguez-Navarro, A. 1995. A potassium transporter of the yeast. *Schwanniomyces occidentalis* homologous to the Kup system of *Escherichia coli* has a high concentrative capacity. *EMBO J.* **14:**3021–3027

Bertl, A., Bihler, H., Kettner, C., Slayman, C.L. 1998. Electrophysiology in the eukaryotic model cell. *Saccharomyces cerevisiae Eur. J. Physiol.* **436:**999–1013

Bertl, A., Ramos, J., Ludwig, J., Lichtenberg-Frate, H., Reid, J., Bihler, H., Calero, F., Martinez, P., Ljungdahl, P.O. 2003. Characterization of potassium transport in wild-type and isogenic yeast strains carrying all combinations of trk1, trk2, and tok1 null mutations. *Mol. Microbiol.* **47:**767–780

Bertl, A., Slayman, C.L. 1992. Complex modulation of cation channels in the tonoplast and plasma membrane of *Saccharomyces cerevisiae*: Single-channel studies. *J. Exp. Biol.* **172:** 271–287

Bertl, A., Slayman, C.L., Gradmann, D. 1993. Gating and conductance in an outward-rectifying K$^+$ channel from the plasma membrane of *Saccharomyces cerevisiae*. *J. Membrane Biol.* **132:**183–199

Bihler, H., Gaber, R.F., Slayman, C.L., Bertl, A. 1999. The presumed potassium carrier Trk2p in *Saccharomyces cerevisiae* determines an H$^+$-dependent, K$^+$-independent current. *FEBS Lett.* **447:**115–120

Blatt, M.R., Rodriguez-Navarro, A., Slayman, C.L. 1987. The potassium-proton symport in *Neurospora:* Kinetic control by pH and membrane potential. *J. Membrane Biol.* **98:**169–189

Blatt, M.R., Slayman, C.L. 1983. KCl leakage from microelectrodes and its impact on the membrane parameters of a nonexcitable cell. *J. Membrane Biol.* **72:**223–234

Blaustein, M., Liberman, M., (eds.) 1984. Electrogenic Transport: Fundamental Principles and Physiological Implications. Raven Press, New York

Bossemeyer, D., Borchard, A., Dosch, D.C., Helmer, G.C., Epstein, W., Booth, I.R., Bakker, E.P. 1989. K$^+$-transport protein TrkA of *Escherichia coli* is a peripheral membrane protein that requires other *trk* gene products for attachment to the cytoplasmic membrane. *J. Biol. Chem.* **264:**16403–16410

Coury, LA., McGeoch, J.E.M., Guidotti, G., Brodsky, J.L. 1999. The yeast *Saccharomyces cerevisiae* does not sequester chloride but can express a functional mammalian chloride channel. *FEMS Microbiol. Lett.* **179:**327–332

Davis-Kaplan, S.R., Askwith, C.C., Bengtzen, A.C., Radisky, D., Kaplan, J. 1998. Chloride is an allosteric effector of copper assembly for the yeast multicopper oxidase Fet3p: an unexpected role for intracellular chloride channels. *Proc. Natl. Acad. Sci. USA.* **95:**13641–13645

Diatloff, E., Kumar, R., Schachtman, DP. 1998. Site-directed mutagenesis reduces the Na$^+$ affinity of HKT1, an Na$^+$ energized high affinity K$^+$ transporter. *FEBS Lett.* **432:**31–36

Durell, S.R., Guy, H.R. 1999. Structural models of the KtrB, TrkH, and Trk1,2 symporters, based on the crystal structure of the KcsA K$^+$ channel. *Biophys. J.* **77:**789–807

Gaber, R.F., Styles, C.A., Fink, G.R. 1986. *TRK1* encodes a plasma membrane protein required for high-affinity potassium transport in *Saccharomyces cerevisiae*. *Mol. Cell. Biol.* **8:**2848–2859

Gassmann, W., Rubio, F., Schroeder, J.I. 1996. Alkali cation selectivity of the wheat root high-affinity potassium transporter HKT1. *Plant J.* **10:**869–882

Gaxiola, R.A., Yuan, D.S., Klausner, R.D., Fink, G.R. 1998. The yeast CLC chloride channel functions in cation homeostasis. *Proc. Natl. Acad. Sci. USA.* **95:**4046–4050

Goldstein, S.A.N., Price, L.A., Rosenthal, D.N., Pausch, M.H. 1996. ORK1, a potassium-selective leak channel with two pore domains cloned from *Drosophila melanogaster* by expression in *Saccharomyces cerevisiae*. *Proc. Natl. Acad. Sci. USA.* **93:** 13256–13261

Greene, J.R., Brown, N.H., DiDomenico, B.J., Kaplan, J., Eide, D.J. 1993. The *GEF1* gene of *Saccharomyces cerevisiae* encodes an integral membrane protein; mutations in which have effects on respiration and iron-limited growth. *Mol. Gen. Genet.* **241:** 542–553

Günther, W., Lüchow, A., Cluzeaud, F., Vandewalle, A., Jentsch, T.J. 1998. CIC-5, the chloride channel mutated in Dent's disease, colocalizes with the proton pump in endocytotically active kidney cells. *Proc. Natl. Acad. Sci. USA.* **95:**8075–8080

Gutknecht, J. 1992. Aspirin, acetaminophen, and proton transport through phospholipid bilayers and mitochondrial membranes. *Mol. Cell Biochem.* **114:**3–8

Gutknecht, J., Tosteson, D.C. 1973. Diffusion of weak acids across lipid bilayer membranes: effects of chemical reactions in the unstirred layers. *Science* **182:**1258–1261

Haro, R., Rodriguez-Navarro, A. 2002. Molecular analysis of the mechanism of potassium uptake through the TRK1 transporter of *Saccharomyces cerevisiae*. *Biochim. Biophys. Acta.* **1564:**114–122

Haro, R., Rodriguez-Navarro, A. 2003. Functional analysis of the M2$_D$ helix of the TRK1 potassium transporter of *Saccharomyces cerevisiae*. *Biochim. Biophys. Acta.* **1613:**1–6

Horie, T., Yoshida, I., Nakayama, H., Yamada, K., Oiki, S., Shinmyo, A. 2001. Two types of HKT transporters with different properties of Na$^+$ and K$^+$ transport in *Oryza sativa*. *Plant J.* **27:**129–138

Huang, M.-E., Chuat, J.-C., Galibert, F. 1994. A voltage-gated chloride channel in the yeast *Saccharomyces cerevisiae*. *J. Mol. Biol.* **242:**595–598

Jennings, M.L., Cui, J. 2003. Chloride transport and homeostasis in *Saccharomyces cerevisiae*. Abstr. 57th Meeting Soc. *Gen. Physiol.* (Woods Hole MA, Sept. 3-7), Item 113 Insert

Kato, Y., Sakaguchi, M., Mori, Y., Saito, K., Nakamura, T., Bakker, E.P., Sato, Y., Goshima, S., Uozumi, N. 2001. Evidence in support of a four transmembrane-pore-transmembrane topology model for the *Arabidopsis thaliana* Na$^+$/K$^+$ translocating AtHKT1 protein, a member of the superfamily of K$^+$ transporters. *Proc. Natl. Acad. Sci. USA.* **98:**6488–6493

Ketchum, K.A., Joiner, W.J., Sellers, A.J., Kaczmarek, L.K., Goldstein, S.A.N. 1995. A new family of outwardly rectifiying potassium channel proteins with two pore domains in tandem. *Nature* **376:**690–695

Kettner, C., Bertl, A., Obermeyer, G., Slayman, C.L, Bihler, H. 2003. Electrophysiological analysis of the yeast V-type proton pump: variable coupling ratio and proton shunt. *Biophys. J.* **85:**3730–3738

Ko, C.H., Buckley, A.M., Gaber, R.F. 1990. *TRK2* is required for low affinity K$^+$ transport in *Saccharomyces cerevisiae*. *Genetics* **125:**305–312

Läuger, P. 1991. *Electrogenic Ion Pumps*. Sinauer Assoc., 313 pp. Sunderland, MA

Lester, H.A., Cao, Y., Mager, S. 1996. Listening to neurotransmitter transporters. *Neuron*. **17:**807–810

Lin, F., Lester, H.A., Mager, S. 1996. Singe-channel currents produced by the serotonin transporter and analysis of a mutation affecting ion permeation. *Biophys. J.* **71:**3126–3135

Liu, W., Schachtman, D.P., Zhang, W. 2000. Partial deletion of a loop region in the high affinity K$^+$ transporter HKT1 changes

ionic permeability leading to increased salt tolerance. *J. Biol. Chem.* **275:**27924–27932

Locke, E.G., Bonilla, M., Liang, L., Takita, Y., Cunningham, K.W. 2000. A homolog of voltage-gated Ca^{2+} channels stimulated by depletion of secretory Ca^{2+} in yeast. *Mol. Cell. Biol.* **20:**6686–6694

Loukin, S.H., Saimi, Y. 1999. K^+-dependent composite gating of the yeast K^+ channel, Tok1. *Biophys. J.* **77:**3060–3070

Mäser, P., Hosoo, Y., Goshima, S., Horie, T., Eckelman, B., Yamada, K., Yoshida, K., Bakker, E.P., Shinmyo, A., Oiki, S., Schroeder, J.I., Uozumi, N. 2002. Glycine residues in potassium channel-like selectivity filters determine potassium selectivity in four-loop-per-subunit HKT transporters from plants. *Proc. Natl. Acad. Sci. USA.* **99:**6428–6433

Minor, D.L., Masseling, S.J., Jan, Y.N., Jan, L.Y. 1999. Transmembrane structure of an inwardly rectifying potassium channel. *Cell* **96:**879–891

Ramos, J., Alijo, R., Haro, R., Rodriguez-Navarro, A. 1994. TRK2 is not a low-affinity potassium transporter in *Saccharomyces cerevisiae. J. Bacteriol.* **176:**249–252

Rodriguez-Navarro, A., Blatt, M.R., Slayman, C.L. 1986. A potassium-proton symport in *Neurospora crassa. J. Gen. Physiol.* **87:**649–674

Rodriguez-Navarro, A., Ramos, J. 1984. Dual system for potassium transport in *Saccharomyces cerevisiae. J. Bacteriol.* **159:**940–945

Röhm, K.-H. 1985. Chloride as allosteric effector of yeast aminopeptidase I. *Arch. Biochem. Biophys.* **239:**216–225

Rubio, F., Gassmann, W., Schroeder, J.I. 1995. Sodium-driven potassium uptake by the plant potassium transporter HKT1 and mutations conferring salt tolerance. *Science* **270:**1660–1663

Rubio, F., Schwarz, M., Gassmann, W., Schroeder, J.I. 1999. Genetic selection of mutations in the high affinity K^+ transporter HKT1 that define functions of a loop site for reduced Na^+ permeability and increased Na^+ tolerance. *J. Biol. Chem.* **274:**6839–6847

Schleyer, M., Bakker, E.P. 1993. Nucleotide sequence and 3′-end deletion studies indicate that the K^+-uptake protein Kup from *Escherichia coli* is composed of a hydrophobic core linked to a large and partially essential hydrophilic C terminus. *J. Bacteriol.* **175:**6925–6931

Schlösser, A., Meldorf, M., Stumpe, S., Bakker, E.P., Epstein, W. 1995. TrkH and its homolog, TrkG, determine the specificity and kinetics of cation transport by the Trk system of *Escherichia coli. J. Bacteriol.* **177:**1908–1910

Schwappach, B., Strobrawa, S., Hechenberger, M., Steinmeyer, K., Jentsch, T.J. 1998. Golgi localization and functionally important domains in the NH_2 and COOH terminus of the yeast CLC putative chloride channel Gef1p. *J. Biol. Chem.* **273:**15110–15118

Sentenac, H., Bonneaud, N., Minet, M., Lacroute, F., Salmon, J.-M., Gaymard, F., Grignon, C. 1992. Cloning and expression in yeast of a plant potassium ion transport system. *Science* **256:**664–665

Sherman, F.C. 1991. Getting started with yeast. *Meth. Enz.* **194:**3–21

Sikorski, R.S., Hieter, P. 1989. A system of shuttle vectors and yeast host strains designed for efficient manipulation of DNA in *Saccharomyces cerevisiae. Genetics* **122:**19–27

Slayman, C.L. 1982. Electrogenic Ion Pumps. *In:* Current Topics in Membranes and Transport. Vol. 16 Academic Press, New-York

Slayman, C.L., Kaminski, P., Stetson, D. 1989. Structure and function of fungal plasma-membrane ATPases. *In:* Kuhn, P.J., (eds) Biochemistry of Cell Walls and Membranes of Fungi. pp 295–312, Springer-Verlag, Berlin

Stumpe, S., Schlösser, A., Schleyer, M., Bakker, E.P., 1996. K^+ circulation across the prokaryotic cell membrane: K^+-uptake systems. *In:* Transport Processes in Eukaryotic and Prokaryotic Organisms. Konings, W.N., Kaback, H.R., Lolkema, J.S. eds. pp 473–500, Elsevier, Amsterdam

Tholema, N., Bakker, E.P., Suzuki, A., Nakamura, T. 1999. Change to alanine of one out of four selectivity filter glycines in KtrB causes a two orders of magnitude decrease in the affinities for both K^+ and Na^+ of the Na^+-dependent K^+-uptake system KtrAB from *Vibrio alginolyticus. FEBS Lett.* **450:**217–220

Uozumi, N., Kim, E.J., Rubio, F., Yamaguchi, T., Muto, S., Tsuboi, A., Bakker, E.P., Nakamura, T., Schroeder, J.I. 2000. The *Arabidopsis* HKT1 gene homolog mediates inward Na^+ currents in *Xenopus laevis* oocytes and Na^+ uptake in *Saccharomyces cerevisiae. Plant Physiol.* **122:**1249–1259

Vergani, P., Miosga, T., Jarvis, S., Blatt, M.R. 1997. Extracellular K^+ and Ba^{2+} mediate voltage-dependent inactivation of the outward-rectifying K^+ channel encoded by the yeast gene *TOK1. FEBS Lett.* **405:**337–344

Vidal, M., Buckley, A.M., Hilger, F., Gaber, R.F. 1990. Direct selection for mutants with increased K^+ transport in *Saccharomyces cerevisiae. Genetics* **125:**313–320

Vidal, M., Buckley, A.M., Yohn, C., Hoeppner, D.J., Gaber, R.F. 1995. Identification of essential nucleotides in an upstream repressing sequence of *Saccharomyces cerevisiae* by selection for increased expression of *TRK2.* Proc. *Natl. Acad. Sci. USA.* **92:**2370–2374

Wada, Y., Ohsumi, Y., Anraku, Y. 1992. Chloride transport of yeast vacuolar membrane vesicles: a study of in vitro vacuolar acidification. *Biochim. Biophys. Acta.* **1101:**296–302

Wadiche, J.I., Amara, S.G., Kavanaugh, M.P. 1995. Ion fluxes associated with excitatory amino acid transport. *Neuron.* **15:**721–728

Walter, A., Hastings, D., Gutknecht, J. 1982. Weak acid permeability through lipid bilayer membranes. *J. Gen. Physiol.* **79:**917–933

Weber, W.-M. 1999. Ion currents of *Xenopus laevis* oocytes: state of the art. *Biochim. Biophys. Acta.* **1421:**213–233

Zeng, G.-F., Pypaert, M., Slayman, C.L. 2004. Epitope tagging of the yeast K^+-carrier, TRK2, demonstrates folding which is consistent with a channel-like structure, J. *Biol. Chem.* **279:**3003–3013